Pilot production of high efficient metal catalyzed textured diamond wire sawed mc-Si solar cells combined with nickel-copper plated front contact processing - SNEC 2017

S. Fox[2a], X. Jie[2b], H. Wu[2c], N. Bay[1d], J. Burschik[1e], W. Dümpelfeld[1f], H. Kühnlein[1g], B. Lee[3h], A. Letize[3i], M. Passig[1i], D. Pysch[1k*], X. Qu[1l], M. Sieber[1m], K. Vosteen[1n]

[1)]RENA GmbH, Hans-Bunte-Strasse 19, 79108 Freiburg, Germany
[2] Jinko Solar, No.58 Yuanxi Road, Yuanhua Industrial Park, Haining, Zhejiang, China 314416
[3)] MacDermid Inc., 245 Freight Street, Waterbury, CT 06702, USA

[a]stephen.fox@jinkosolar.com, [b]xiaodong.jie@jinkosolar.com, [c]huimin.wu@jinkosolar.com, [d]norbert.bay@rena.com, [e]john.burschik @rena.com, [f]wolfgang.duempelfeld@rena.com [g]holger.kuehnlein@rena.com,[h]blee@macdermidenthone.com, [i]aletize@macdermidenthone.com, [j]michael.passig@rena.com, [k]damian.pysch@rena.com, [l]xiaobin.qu@rena.com, [m]markus.sieber@rena.com, [n]konrad.vosteen@rena.com

Abstract: This paper presents first results of combining two promising future technologies: i) metal catalyzed textured diamond-wire sawn (DWS) mc-Si wafering and ii) nickel-copper-silver (Ni/CuAg) plated front contact processing. Results of first optimizations of laser patterning, annealing and module string soldering are presented. A 60-cell module with a power output of 266 W has been successfully manufactured. The pseudo fill-factor (pFF) has been identified as the parameter with the highest potential for further improvements. A very promising approach is moving from an emitter profile that is mainly adapted to silver paste properties to an optimized emitter profile for Ni/Cu/Ag-plated contacts. The idea is to reduce the surface doping concentration (reduces Auger-recombination) and increase the junction depth (increased pFF and FF).

Keywords: Cu-plating; Light-induced plating; Diamond-wire saw, multi-crystalline texture, metal catalyzed texture

* Corresponding author. Tel.: +4916090448525;
E-mail address: damian.pysch@rena.com

1 Introduction

In the past decade, the PV industry undertook considerable efforts to make Si solar cells cost effective relative to conventional carbon emitting energy generation technologies (coal, gas etc.). This goal has been achieved for several regions in the world [1]. Now, due to production overcapacity, the continued and increased pressure to further reduce production costs is driving all promising innovations (both disruptive and evolutionary). One important innovation step in the past year was the replacement of slurry-wire-based wafer sawing technology with diamond-wire-based wafer sawing technology for cast multi-crystalline (mc-Si) wafers. Amongst other improvements, this was one main step to improve the cost advantage of mc-Si wafers compared to Cz-Si-wafers. On one hand, many solar cell producers are switching their production from mc- to Cz-wafer based silicon solar cells, because wafer costs per watt currently favor Cz-Si wafers [2]. On the other hand, different approaches are being investigated to cost-effectively texture diamond wire saw (DWS) mc-Si wafers. The common acidic HNO_3/HF-based texture process, optimized for slurry-wire sawn mc-Si wafers cannot be applied conveniently to DWS mc-Si wafers. One very promising approach is with so-called metal catalyzed texturing (MCT) technology. Its process details, electrical performance and feasibility for combination with Ni/Cu/Ag-plating is discussed in detail in the following sections of this paper.

A second, very promising approach to significantly reduce production costs is the substitution of cost-intensive screen-printed Ag-pastes with Ni/Cu/Ag-plating [3]. Furthermore, copper plating technology comes along with a potential to increase the efficiency by 0.1 to 0.3% absolute compared to the current screen-printing technology. Due to silver's roles as both a semi-precious investment metal and as an industrial commodity, silver paste prices are highly sensitive to volatile speculative trends in metals exchange markets, which in turn has the undesirable effect of shrinking the already-narrow margins of most solar cell manufactures. Replacing the Ag paste with a low-cost price-stable plated Ni/Cu/Ag stack would alleviate this cost pressure. Another important consideration is that due to the limited known-reserves of silver, it will certainly become a bottleneck in the scale-up of the PV technology as it seeks to play a more-significant role in the global power generation market [4]. Last, but not least, a copper-plated silicon solar cell would fit the broader commercial market's demand of abandoning lead, a toxic component of silver metallization pastes, from the device.

Thus, the two most cost-intensive factors in Si wafer-based solar cell production (wafer and metallization) are tackled by the following presented work.

2 Process and equipment

2.1 Solar cell processing

The following process flow was applied to all solar cells subsequently described herein: After obtaining wafers by diamond-wire sawing of the cast mc-Si ingot, an MCT surface texturing process as depicted in Fig. 2 was applied. The MCT process is discussed in more detail in section 2.2. Next, a shallow 100-Ω/□ phosphorous-doped emitter was formed via thermal diffusion of $POCl_3$ (see Fig. 5, as formed). After this, PSG is etched from the cell surfaces and the junction is isolated by single-side silicon etch. Then, a SiN_x anti-reflection coating was deposited by tube PECVD on the front-side. On the rear-side, Al-paste (for Al-BSF formation)

and silver pads (for cell inter-connection) was printed and fired for all Ni/Cu/Ag contacted solar cells. For the reference cells, an Ag-paste was screen-printed on the front side before firing. This comparison of metallization process flows is illustrated in Fig.1.

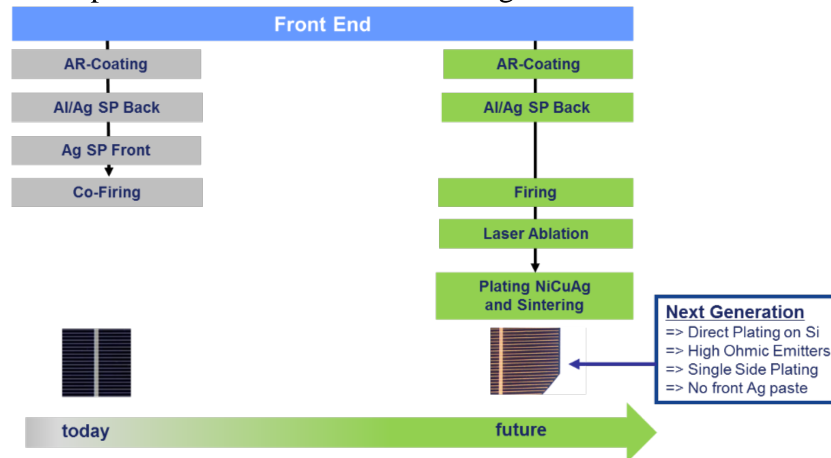

Fig 1: Process flow overview for conventional solar cells with screen-printed silver front-side contact metallization (left) and solar cells with laser-patterned, plated Ni/Cu/Ag contact metallization, and sintering (right).

2.2 Metal-catalyzed texturing of diamond-wire sawn multi-crystalline Si-wafers

The process flow for metal-catalyzed texturing of diamond-wire sawn multi-crystalline Si-wafers is shown in Figure 2a. First, the DWS mc-wafers are treated with an alkaline damage-removal etch (DRE), followed by the actual MCT process, which can be sub-divided into a metal deposition step and an acidic etching step [5,6]. Next, an acidic damage-removal step is applied, followed by an alkaline clean and then an acidic clean. In-between all process steps, a rinse needs to be conducted. Application of this process chain to DWS mc-Si wafers results in surface morphologies as shown in Fig. 2 b).

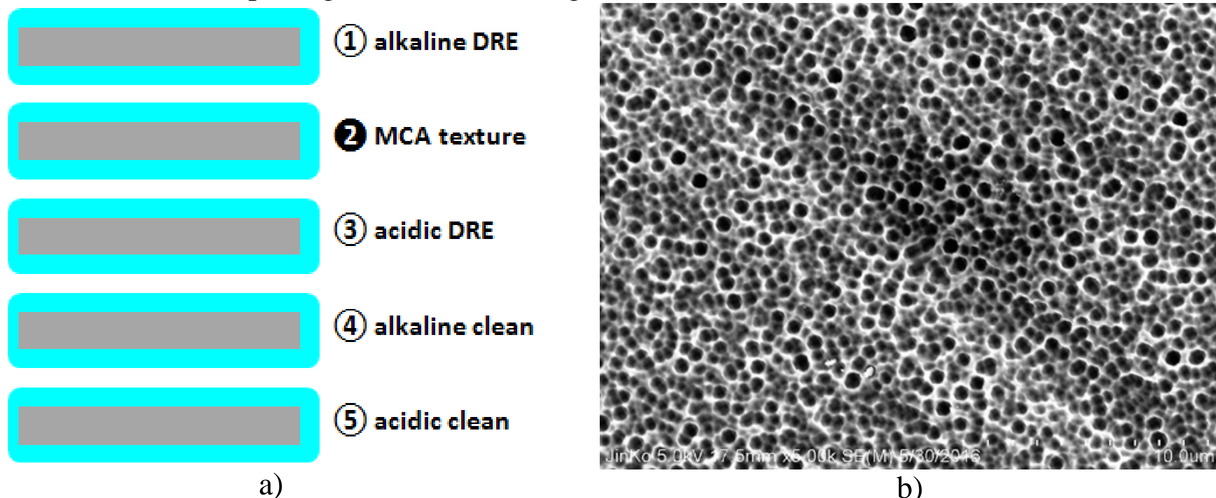

Fig 2: a) process overview for the MCT process, b) representative image of MCT-textured DSW mc-Si wafer surface.

2.3 Ni/Cu/Ag plating process

In order to deposit Ni/Cu/Ag-plated contacts, the contact pattern needs to be formed by selective UV-ps laser ablation of the front PECVD SiNx:H layer. The subsequent in-line plating relies on single-sided wet chemical processing in order to protect the rear contacts of the solar cells. The in-line plating process starts with a chemical pre-treatment of the laser-opened areas,

to assure plating will start on the exposed emitter surface where intended. Nickel (Ni) is plated by light-induced plating (LIP). A Cu layer is then plated on top of Ni, to give the contacts sufficient conductivity (see Fig. 3b) and c)). At the end of the plating sequence, single-sided immersion plating of Ag caps the Cu layer. This very thin (100-nm, or less) Ag layer prevents Cu oxidation and facilitates soldering of interconnection ribbons to the metal stack (see Fig. 3a). The laser step was performed on a Innolas equipment and all plating steps are performed with RENA-manufactured in-line equipment in conjunction with MacDermid-Enthone-produced plating chemistry. Intermediate rinsing and drying steps are applied in-between all process baths. In a last processing step, the complete metal stack is thermally annealed in an inert atmosphere. During this step, the adhesion of the metal stack to Si is improved and the contact resistance and line resistance are reduced via appropriate nickel-silicide formation at the nickel-silicon interface [7].

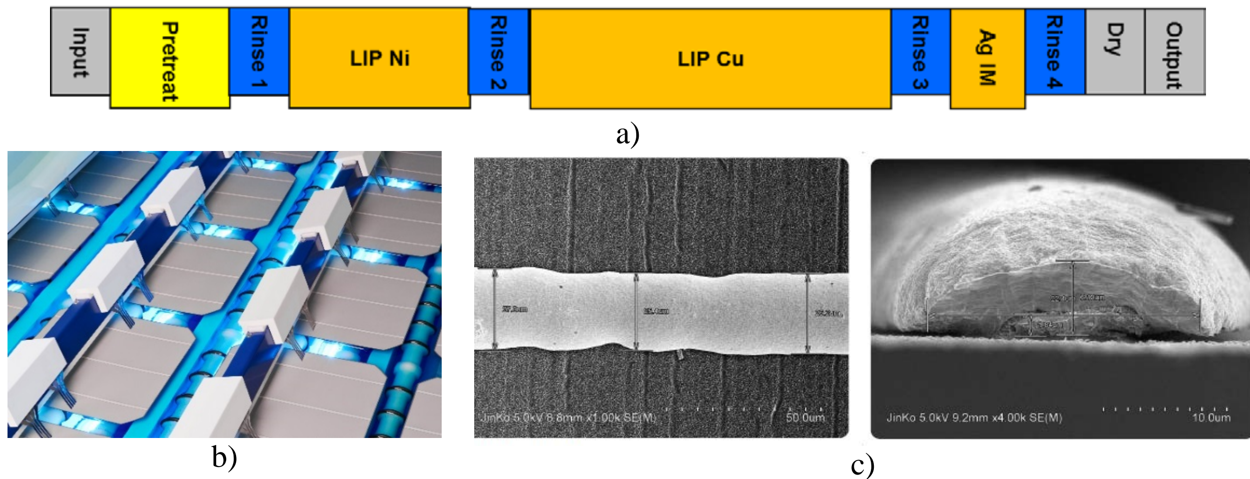

Fig 3: a) Sketch of Ni/Cu/Ag plating process flow, b) picture of light-induced plating LIP Cu process bath, c) representative SEM image of plated contact finger on a MCT DWS-Si-wafer. Left: top view of a 22-µm wide finger is shown. Right: cross-section of the same contact finger with a finger height around 10-µm is shown.

3 Experimental work

In order to achieve an efficiency increase with plated cells relative to Ag-paste screen printed cells, some processes steps have to be individually optimized [8].

3.1 Laser processing and influences on solar cell performance

First, the laser process was optimized to the MCT wafer surface. The goal is to realize a homogenous opening in the SiN_x layer while simultaneously minimizing the creation of a laser-induced damage region (specifically, silicon amorphization) within the emitter's crystal structure. In Figure 4 a), mean efficiency values (5 cells per group) before and after annealing are shown over varied laser pulse energies. A wide process window, between 0.6 to 0.8 µJ/pulse, results in high efficiencies above 19%. No significant difference of the investigated dependency can be distinguished before and after the anneal process, aside from an increase in efficiency by approximately 0.2%. In Figure 4 b), a representative surface image after laser patterning is shown for the optimum laser parameter of 0.8 µJ/pulse.

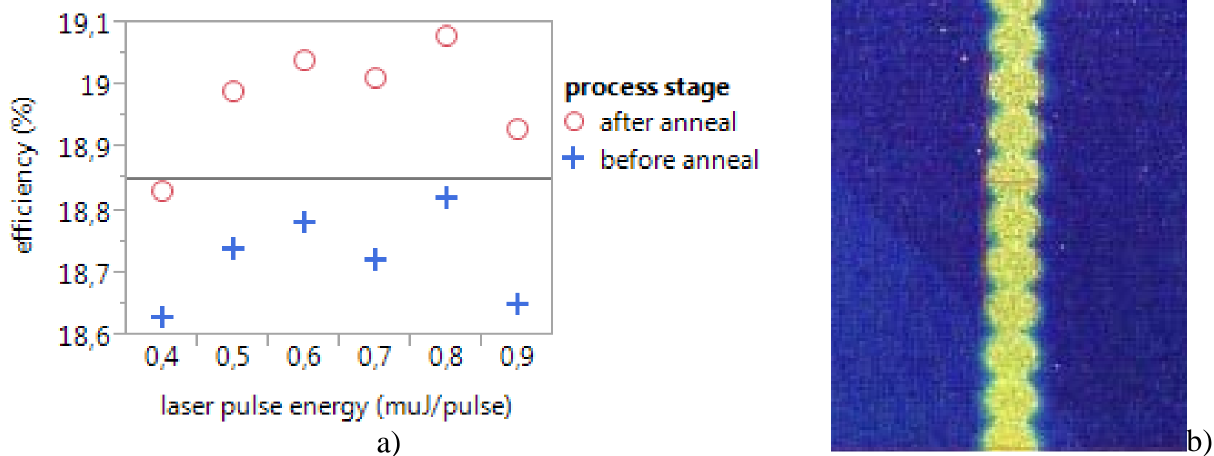

Fig 4: a) mean efficiency values (5 cells per group) before and after annealing over normalized laser power is shown. b) Representative surface image after laser patterning.

In Figure 5 a comparison of emitter doping profiles before and after laser ablation for three different normalized laser power settings (0.5, 0.7, and 0.9 µJ/pulse), is presented. The laser process only influences the emitter profile to a depth of approximately 50-nm. The emitter depth below 50-nm is only marginally influenced. Thus, no strong laser damage is induced during laser patterning of MCT mc-Si wafers. However, since the emitter terminates at a shallow depth of approximately 200 nm, and considering that during the annealing process the Ni-layer at the interface forms a Ni-silicide with the emitter layer, it can be reasoned that a deeper junction depth might be beneficial for further efficiency increase. It is important to note that the emitter profile shown in Figure 5 is optimized for Ag-silver paste only and does not reflect the optimum emitter profile for maximizing the solar cell performance for a plated cell. A profile with a reduced surface concentration and a deeper junction would lead to higher efficiencies since the Auger-Recombination could be reduced.

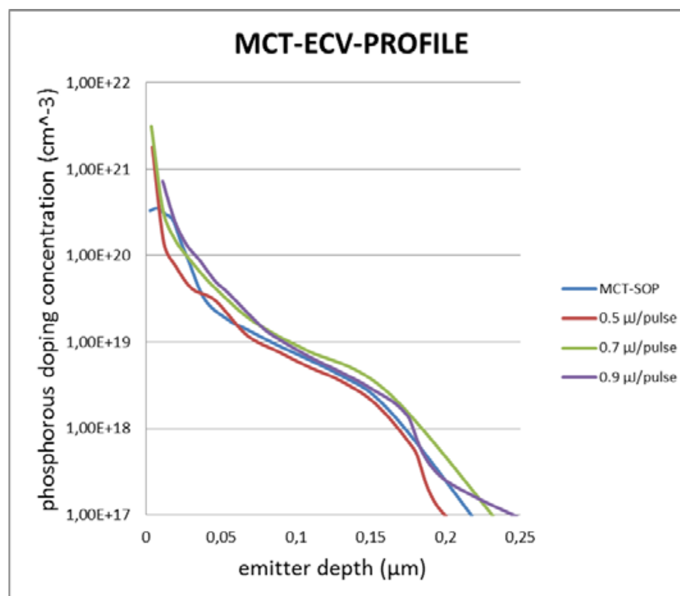

Fig 5: Comparison of emitter doping profiles before and after laser ablation for three different normalized laser power setting (0.5, 0.7, and 0.9 µJ/pulse).

3.2 Influence of annealing process

In Figure 6 a), the influence of the annealing temperature on the efficiency is shown for two different annealing durations: 3-min and 6-min. The efficiency is quite stable between 18.8% and 19.0% for annealing temperatures between 300°C and 375°C. For higher temperatures, the efficiency drops rapidly. No significant difference is observed between 3-min and 6-min annealing times. Thus, in the future, a 3-min anneal time will be considered as optimal. In Figure 6 b), the contact resistivity is shown as a function of annealing temperature (3-min). A good match to the I-V data is demonstrated. For temperatures below 400°C, very low contact resistivity values are observed. Above 400°C, the contact resistance rises rapidly. This finding is in good agreement with observation in [9]

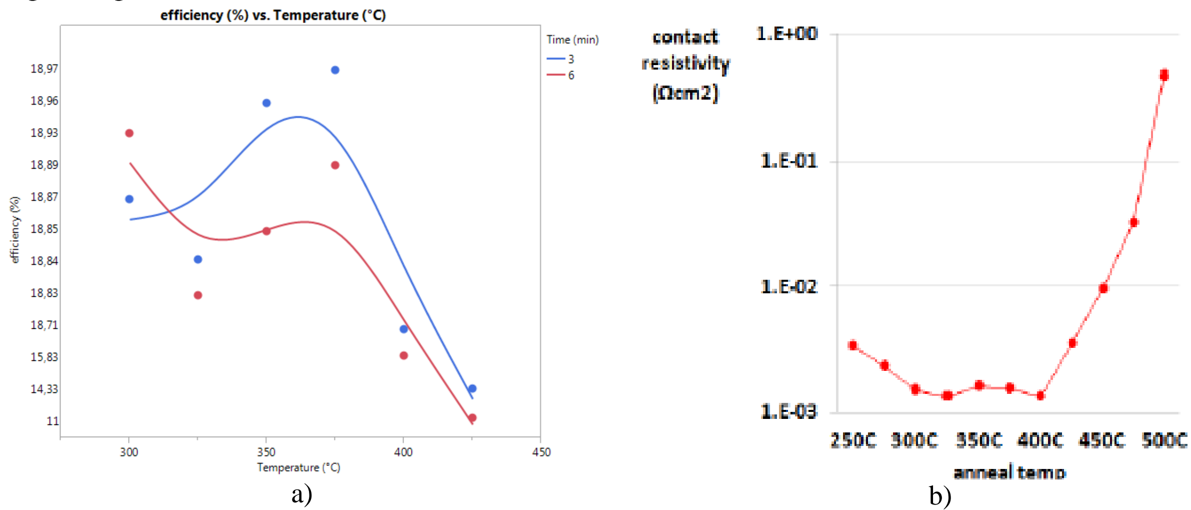

a) b)

Fig 6: a) Efficiency over annealing temperature is shown for two different durations 3 and 6 min. b) Contact resistivity over annealing temperature (3 min) is shown.

3.3 I-V data comparison of MCT mc-Si solar cells contacted by silver paste screen-printing vs. Ni/Cu/Ag-plating

After the initial process development (process 'base-lining') cycle, as described in section 3.1 and 3.2, two groups (10 cells each) of cells are fabricated in order to compare the electrical performance of the plated Ni-Cu-Ag contact technology to conventional screen-printed Ag-paste contact technology. The I-V data is shown in Table 1. The efficiency for the plated front contact group is slightly higher. The main reasons for this are a superior short circuit current (J_{sc}) and FF. The higher FF is mainly explained by a significantly reduced series resistance (R_s) value. Based on the observed R_s difference, an even higher advantage in FF should be observed [10]. Based on this observed difference, it is reasoned that the plated group has a reduced pseudo fill factor. This finding leads to the conclusion that the diode quality of the plated cells is most likely reduced either by a laser-induced emitter damage, a too-shallow junction, Ni-silicide spiking after anneal, or a combination of the above-mentioned influences.

Tab. 1: Overview of I-V data (efficiency, V_{oc}, J_{sc}, FF, and R_s) for two different front contact metallization: i) Ni/Cu/Ag plating (after annealing), and ii) Ag-paste screen printing. The group size is 10 cells per group.

Group	η (%)	V_{oc} (mV)	J_{sc} (A)	FF (%)	R_s (mΩ)
Ni/Cu/Ag plated MCT cells	19,04	637	9,11	80,37	1,3
Ag screen printed MCT cells	19,00	642	8,99	80,12	2,1

4 Module results

Before committing to the fabrication of a full-sized 60-cell module the feasibility of Ni/Cu/Ag-plated MCT mc-Si cells to standard solder technology for interconnecting 12 cells in a string is investigated. In Figure 7, the observed failure pull strength forces, after standard module-production contact tab soldering is performed, are shown. All values were determined under a pull angle of 60°. The contact annealing temperature and time has been varied from 300°C to 450°C and 3-min to 6-min, respectively. Values above 1-N are known to allow for a reliable module production process. Longer annealing times performs slightly better compared to the 3-min anneal, with most values well above 2-N. It is known that the solderability of plated Ag on Cu is much higher than on Ag paste. Optimization of the soldering process will be part of future experiments.

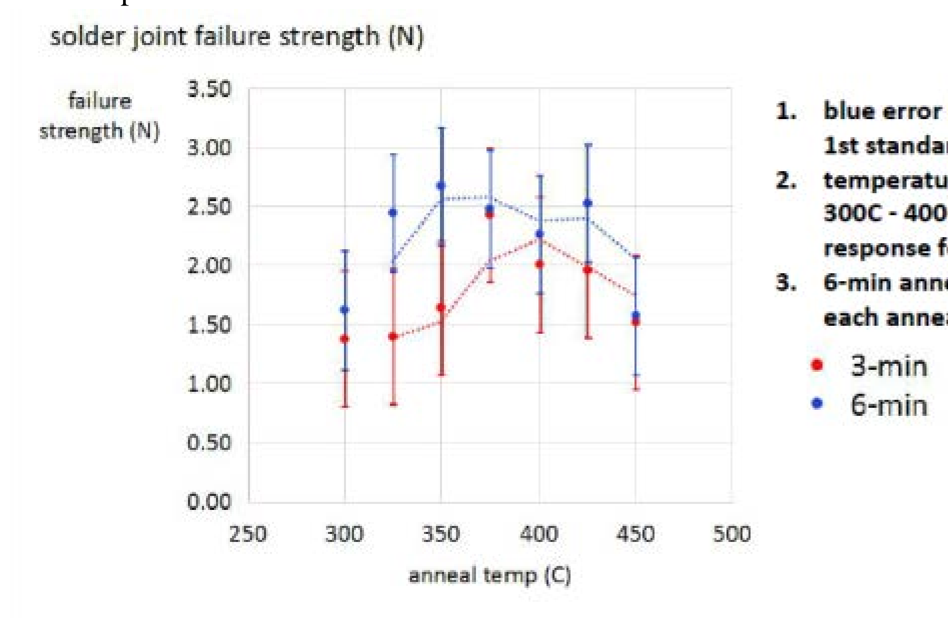

Fig 7: Measured failure pull strength force after standard contact tab soldering for module production. All values were determined under a pull angle of 60°. The contact annealing temperature and time has been varied from 300°C to 450°C and 3-min to 6-min, respectively.

After obtaining positive results, as discussed in sec. 3.3 and shown in Fig.7, 225 cells were fabricated (see I-V data distribution in Fig 8a)) and a 60-cell module was subsequently manufactured. The module electro-luminescence (EL) image is shown in Fig.8b). Please note that despite no adaptation of the cell interconnection or the module 'lay-up' processes to the presence of plated bus bar pads, neither cell cracks, nor finger interruptions, nor other typical module failure modes are observed through visible inspection of the EL image. The module I-V data is show in Figure 8c). The power output accounts 266W. After further optimization loops are completed, modules in the output range of 280-W to 290-W are expected.

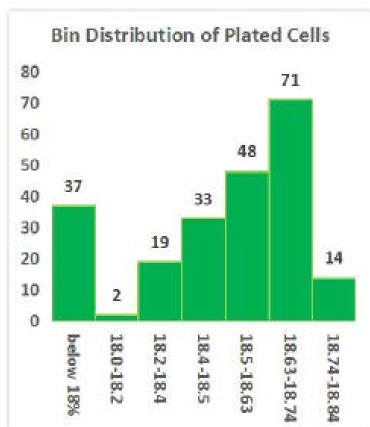

a)

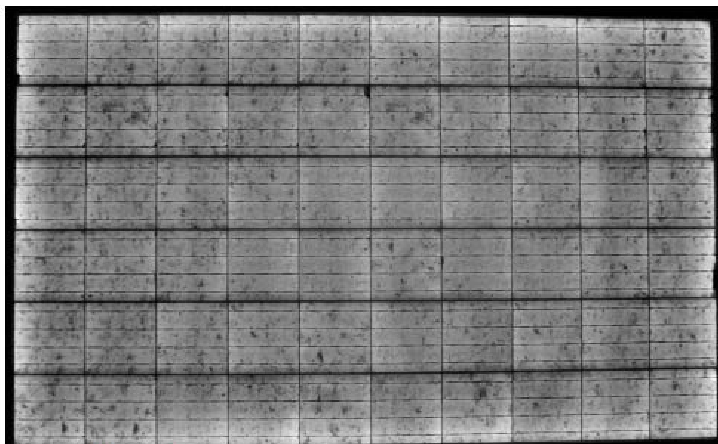

b)

c)

Fig 8: a) Efficiency binning distribution of 225 MCT mc-Si solar cells contacted by a plated Ni/Cu/Ag stack. b) EL image and c) I-V data of a very first 60-cell module populated with cells shown in Fig. 8a).

4 Conclusion and outlook

Within this publication, we present the case that combining two emerging technologies, specifically, metal catalyzed textured diamond wire saw mc-Si wafering and Ni/Cu/Ag-plated front contact processing, shows very good results, even at the process 'base-lining' stage of development. Results from the initial rounds of unit-process optimization, including laser patterning, annealing, and soldering are presented.

A 60-cell module with a power output of 266-W has been presented with fabrication of 280-W to 290-W modules, along with subsequent generation of module reliability data, as 'next-steps'. Since unit-process development and whole-process integration are in the early stages, it is expected that further optimizations will result in rapid near-term improvement in cell and module performance. As a primary case-in-point, discussed in sec. 3.3, is that the plated cell's I-V response mainly suffers due to a reduced pFF. A very promising solution for this is

moving away from an emitter profile which is mainly optimized for silver paste's restricted sintering parameters and, thus, limited contacting properties and, instead, developing an optimized emitter profile suited for highly-ohmic Ni/Cu/Ag-plated contacts. The main idea is to reduce the surface doping concentration (reduces Auger-recombination) and increase the junction depth (increased pFF and FF). In Figure 9 the conventional Ag-paste influenced emitter profile and a proto-type plating-optimized emitter are shown. Initial I-V results are imminent.

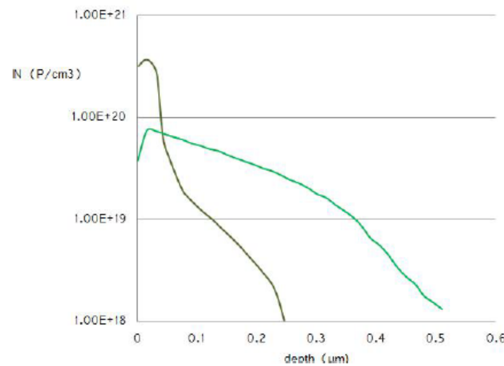

Fig 9: Comparison of n-type Emitter profiles on MCT mc-Si cells: a) current profile which is optimized for Ag-paste screen-printing, b) proto-type emitter profile optimization for Ni/Cu/Ag front-contact formation.

References

[1] Lazard, " Lazard's levelized cost of energy analysis – Version 10.0" December 2016 www.lazard.com/media/438038/levelized-cost-of-energy-v100.pdf (10.4.2017)

[2] SEMI PV Group Europ 2016, "IRTPV Eight Edition 2017" www.itrpv.net/reports/downloads/ (10.4.2017)

[3] J. Horzel, Y. Shengzhao, N. Bay, M. Passig, D. Pysch, H. Kühnlein, H. Nussbaumer, P. Verlinden, „Industrial Si solar cells with Cu-plated contacts," IEEE J. Photovolt., vol. 5, no. 6, pp. 1595-1600, Nov. 2015

[4] Meng Tao; "Terawatt Solar Photovoltaics: Roadblocks and Opportunities" Springer Verlag 2014, DOI 10.1007/978-1-4471-5643-7

[5] Xiaoya Ye, Shuai Zou, Kexun Chen, Jianjiang Li, Jie Huang, Fang Cao, Xusheng Wang, Lingjun Zhang , Xue-Feng Wang , Mingrong Shen , and Xiaodong Su; "18.45%-Efficient Multi-Crystalline Silicon Solar Cells with Novel Nanoscale Pseudo-Pyramid Texture" Adv. Funct. Mater. 2014, 24, 6708–6716

[6] X. Wang, S. Zou, G. Xing, „19,31% efficient multicrystalline silicon solar cells using MCCE black silicon technology" Photovoltaics International 35th Edition, 02/2017

[7] R. Russel, L. Tous, H. Philipsen, J. Horzel, E. Cornagliotti, M. Ngamo, P. Choulat, R. Labie, J. Bekcers, J. Bertens, M. Fujii, J. John, J. Poortmans, R. Mertens „a simple copper metallization process for high cell efficiencies and reliable modules", Proceedings of 27th EUPVSEC, Frankfurt, Germany, 2012

[8] Norbert Bay, Andreas A. Brand, Andreas Büchler, John Burschik, Sven Kluska, Holger H. Kuehnlein, Michael Passig, Damian Pysch, Markus Sieber „Benefits of different process

routes for industrial direct front side plating" 7th International Conference on Silicon Photovoltaics, SiliconPV 2017

[9] T. Murakami, B. Froment, M. Ouaknine, W. Yoo, "Nickel silicide formation using a stacked hotplate based low temperature annealing system" Presented at 203rd Electrochemical Society Meeting in Paris (May, 2003)

[10] D. Pysch, A. Mette, S.W. Glunz, A review and comparison of different methods to determine the series resistance of solar cells, Sol. Energy Mater. Sol. Cells 91 (2007) 1698–1706.